

Dynamic conformational changes in the FERM domain of FAK are involved in focal-adhesion behavior during cell spreading and motility

Ekaterina Papusheva¹, Fernanda Mello de Queiroz¹, Jeremie Dalous², Yunyun Han¹, Alessandro Esposito³, Elizabeth A. Jares-Erijman^{4,5}, Thomas M. Jovin^{5,6} and Gertrude Bunt^{1,2,5,*}

¹Molecular Biology of Neuronal Signals, Max-Planck Institute of Experimental Medicine, 37075 Göttingen, Germany

²Department of Neuro- and Sensory Physiology, University Medicine Göttingen, 37073 Göttingen, Germany

³Cellular Biophysics, European Neuroscience Institute, 37073 Göttingen, Germany

⁴Departamento de Química Orgánica, Facultad de Ciencias Exactas y Naturales, Universidad de Buenos Aires, Buenos Aires, Argentina

⁵DFG Research Center for Molecular Physiology of the Brain (CMPB), 37073 Göttingen, Germany

⁶Laboratory of Cellular Dynamics, Max-Planck Institute for Biophysical Chemistry, 37077 Göttingen, Germany

*Author for correspondence (e-mail: gbunt@gwdg.de)

Accepted 6 November 2008

Journal of Cell Science 122, 656–666 Published by The Company of Biologists 2009

doi:10.1242/jcs.028738

Summary

Focal adhesion kinase (FAK) controls cellular adhesion and motility processes by its tight link to integrin- and extracellular-matrix-mediated signaling. To explore the dynamics of the regulation of FAK, we constructed a FRET-based probe that visualizes conformational rearrangements of the FERM domain of FAK in living cells. The sensor reports on an integrin-mediated conformational change in FAK following cellular adhesion. The perturbation is kinase-independent and involves the polybasic KAKTLR sequence in the FERM domain. It is manifested by an increased FRET signal and is expressed primarily in focal adhesions, and to a lesser extent in the cytoplasm. The conformational change in the FERM domain of FAK is observed in two consecutive phases during spreading – early and late – and is enriched in fully adhered motile cells at growing and sliding peripheral focal-adhesion sites, but not

in stable or retracting focal adhesions. Inhibition of the actomyosin system indicates the involvement of tension signaling induced by Rho-associated kinase, rather than by myosin light-chain kinase, in the modulation of the FERM response. We conclude that the heterogeneous conformation of the FERM domain in focal adhesions of migrating cells reflects a complex regulatory mechanism for FAK that appears to be under the influence of cellular traction forces.

Supplementary material available online at
<http://jcs.biologists.org/cgi/content/full/122/5/656/DC1>

Key words: FERM conformation, FAK, FRET, Migration, ROCK, Force

Introduction

Cell adhesion and migration are essential processes for embryonic development, wound healing and inflammation, and are pathologically involved in tumor invasion and metastasis. Proper migration requires the coordinated adhesion and detachment of cells from the extracellular matrix (ECM) (Lauffenburger and Horwitz, 1996; Ridley et al., 2003). In a typical migration cycle, adhesive focal complexes that are formed at the leading edge mature into focal adhesions (FAs) that pull the cell forward, followed by their release at the rear. For the execution of an adequate and directed migration response, numerous cellular inputs need to be coordinated. These principally involve adhesion signals mediated by integrin receptors, and modulation of these signals by chemotactic cues.

The mechanisms by which adhesive signals are translated into cellular responses are only now beginning to be understood. The engagement of integrins with the ECM results in their clustering and the formation of focal complexes and adhesions by the recruitment, binding and activation of downstream signaling proteins (BurrIDGE and FATH, 1989). Thus, integrins not only act as simple structural components but actually transduce biochemical signals across the cell membrane.

Focal adhesion kinase (FAK) is a 125-kDa non-receptor tyrosine kinase that is recruited to FAs and activated by integrins (Mitra et al., 2005). As a key mediator of integrin signaling, FAK performs executive and regulatory roles in cell adhesion and migration, yet our understanding of its activity regulation during these processes remains incomplete. FAK knockout in mice is embryonically lethal (Furuta et al., 1995), and cells derived from such embryos fail to induce FA growth and exhibit reduced migration (Ilic et al., 1995). The essential role of FAK in cell migration is well documented (Gilmore and Romer, 1996; Owen et al., 1999; Sieg et al., 1999). In particular, FAK is involved in the regulation of FA dynamics (Ezratty et al., 2005; Hamadi et al., 2005; Schober et al., 2007; Sieg et al., 1999; Webb et al., 2004) and in the spatial organization of the leading edge in migrating cells (Tilghman et al., 2005).

FAK consists of a central kinase domain (KD) flanked by regulatory regions. The N-terminal region contains the FERM domain, which shares homology and structural similarity with the band 4.1 and ezrin-radixin-moesin (ERM) proteins (Ceccarelli et al., 2006; Girault et al., 1999). The FERM domain mediates crosstalk with chemotactic pathways by interaction with activated growth-factor receptors (Chen and Chen, 2006; Sieg et al., 2000). The

C-terminus includes a proline-rich domain and the FA-targeting (FAT) domain (Arold et al., 2002; Hayashi et al., 2002).

FAK is recruited to FAs by binding to the integrin-associated proteins paxillin (Tachibana et al., 1995) and talin (Chen et al., 1995), resulting in FAK activation and autophosphorylation at Tyr397 (Calalb et al., 1995; Kornberg et al., 1992; Schaller et al., 1994). Tyr397 is the major phosphorylation site of FAK. Its phosphorylation creates a Src homology 2 (SH2)-binding site that can bind various interaction partners, including Src-family kinases, PI3-kinase and Grb7 (Han and Guan, 1999; Reiske et al., 1999; Schaller et al., 1994; Schlaepfer and Hunter, 1996). In turn, binding and subsequent activation of the Src kinase results in phosphorylation of FAK at its 'downstream' residues, Tyr576 and Tyr577, and maximal kinase activation (Calalb et al., 1995; Ruest et al., 2000). Moreover, Src phosphorylation of FAK at Tyr863 facilitates the binding of p130Cas (Lim et al., 2004) and Grb2 (Schaller et al., 1994; Schlaepfer and Hunter, 1996), and phosphorylation of Tyr925 promotes the binding of Grb2 (Schlaepfer et al., 1998). The FAK-interacting proteins initiate downstream cell-migration signaling pathways, primarily involving the Rho-family GTPases (Chen et al., 2002; Hsia et al., 2003; Ren et al., 2000; Wu et al., 2004; Zhai et al., 2003) and the Ras-MAP-kinase cascade (Hanks et al., 2003).

In addition to phosphorylation, there is compelling evidence that FAK activity is regulated by structural rearrangements involving the FERM domain. Deletion of the FERM domain leads to hyperphosphorylation, i.e. activation of FAK in suspended cells, and renders its activity independent of Src (Cooper et al., 2003; Jacamo and Rozengurt, 2005). It has been suggested that integrin-mediated activation of FAK releases an auto-inhibitory interaction of the FERM domain with the KD. The point mutation Lys38AAla (K38A) in the FERM domain presumably weakens the interaction between the domains, inasmuch as it leads to FAK hyperphosphorylation, increases cell motility and facilitates cell-cycle progression (Cohen and Guan, 2005). It has been proposed that the FERM domain is involved in yet another interaction – one required for maximal kinase activation and for promoting cell adhesion and migration (Dunty et al., 2004). This interaction involves a polybasic sequence (KAKTLR) at the tip of the FERM

F2 lobe. The crystal structure of the FERM-KD fragment of FAK reveals that the FERM domain directly binds the kinase domain when FAK is in its inactive state, thereby blocking access to the catalytic cleft and preventing Tyr397 autophosphorylation and Src-mediated phosphorylation of the activation loop (Lietha et al., 2007).

Despite abundant data on FAK activation, an understanding of its regulation in cells is still lacking, particularly with respect to the dynamically orchestrated adhesion properties of the migrating cell. FAK becomes rapidly activated during cell spreading on the ECM when new focal contacts are formed (Schaller et al., 1994; Schlaepfer et al., 1998). Conversely, FAK recruitment and activity is also associated with FA disassembly (Ezratty et al., 2005; Hamadi et al., 2005; Webb et al., 2004). How FAK is regulated to transduce these opposing cellular responses remains to be elucidated.

In order to resolve the many issues raised above, it is important to better characterize at the molecular level how FAK function relates to FA behavior. Here, we used a FRET-based biosensor that allows a spatially and temporally resolved visualization of FERM conformational changes during integrin-mediated regulation of FAK. The sensor provides new insights into the involvement of FAK in the heterogeneous behavior of FAs during early cell spreading and motility.

Results

Construction of a FRET-based sensor for FAK conformational changes

In order to investigate adhesion-associated conformational rearrangements in the FAK molecule, we constructed an intramolecular FRET-based sensor. The phenomenon of FRET, the radiationless transfer of excited-state energy between fluorophores, is ideally suited for the study of conformational changes (Bunt and Wouters, 2004). In initial exploratory experiments, we determined that the large size of FAK (125 kDa) prevented the occurrence of FRET in FAK that was labeled at both termini with the donor-acceptor pair ECFP-EYFP (Fig. 1A). We decided to increase the probability of FRET coupling by placing one of the fluorophores inside the coding sequence of FAK, such that it would sense conformational changes relative to the second, terminal, fluorophore.

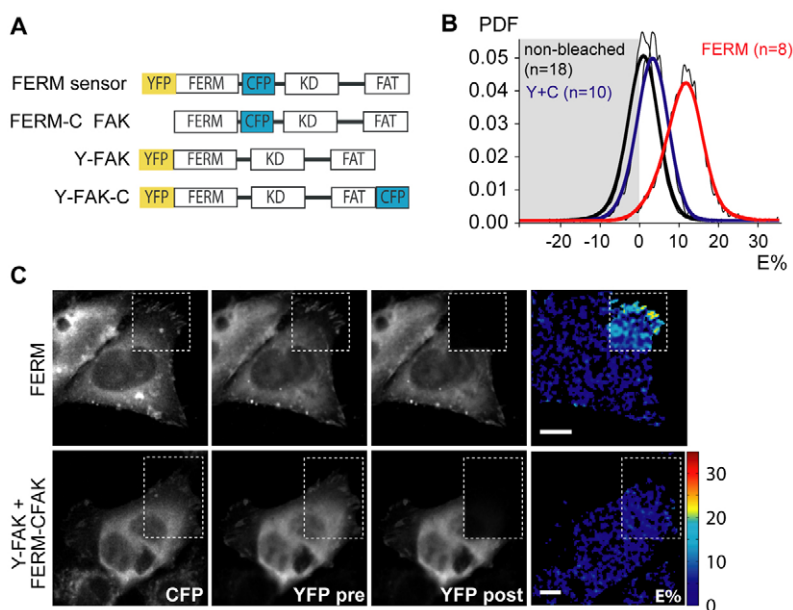


Fig. 1. The FERM sensor reports on an intramolecular conformational change in the FERM domain of FAK. (A) Overview of the FAK-FRET probes used. In the FERM sensor, CFP (donor) is inserted at site 391 to measure FRET with YFP (acceptor) at the N-terminus. (B,C) FRET-efficiency ($E\%$) distributions of the FERM sensor compared with co-transfected singly labeled Y(FP)-FAK and FERM-C(FP) FAK constructs in *FAK*^{-/-} fibroblasts as detected by acceptor photobleaching. (B) Cumulative histograms (as probability density functions, PDF) of the measured FRET-efficiency distributions over the indicated number of cells (n). (C) FRET-efficiency images of representative cells. YFP pre and YFP post indicate YFP fluorescence intensities before and after photobleaching, respectively. YFP was bleached in the boxed area. FRET efficiencies are displayed in pseudo-color scale as indicated. Scale bars: 10 μm .

To obtain sensors for structural rearrangements of the FERM domain, we searched for conformationally sensitive and insertion-tolerant sites in the FERM domain and in the connecting linker to the kinase domain. Using Tn5-transposase random-insertion cloning, we generated a library of FAK constructs with randomly inserted sequences that could be targeted for fluorescent labeling (Sheridan et al., 2002). Clones carrying insertions in the FERM domain or in its linker were selected. The inserted ampicillin-resistance gene was replaced by ECFP, and EYFP was fused at the N-terminus. The FRET constructs were screened for correct FA localization and morphology in HeLa cells and *FAK*^{-/-} fibroblasts.

The conformationally responsive regions of the FERM domain of the constructs were probed in adherent *FAK*^{-/-} fibroblasts by FRET measurements using acceptor photobleaching (Jares-Erijman and Jovin, 2006). The construct showing the greatest FRET contrast between cytosol and FAs was selected for further study (clone 153). CFP was inserted after amino acid Val391, i.e. in the linker between the SH3 Src-binding site (amino acids 368-375) and the Tyr397 phosphorylation site (Fig. 1A). This YFP-FAK153-CFP construct is hereafter referred to as the 'FERM sensor'. The FERM sensor exhibited significant FRET, with an overall mean efficiency of 12% (Fig. 1B). FRET efficiencies between FAs and the cytosol were different, with considerably higher efficiencies in the FAs, reaching up to 25-30% (Fig. 1C, upper panel). Such a differential distribution of FRET suggests adhesion-dependent conformational changes in the FERM domain.

In order to exclude the occurrence of FRET due to dimerization of separate sensor constructs, we coexpressed singly donor-labeled FAK153-CFP and acceptor-labeled YFP-FAK constructs (Fig. 1B,C) in *FAK*^{-/-} fibroblasts to prevent the dilution of a FRET signal by the participation of endogenous FAK in dimerization. We excluded from our analysis those cells that did not attain an acceptor:donor molecular expression ratio of at least 1:1, thus favoring a maximal extent of FRET exchange between the constructs. The measured FRET efficiency upon coexpression of the singly labeled FAK constructs was negligible ($1.9 \pm 3.2\%$ vs non-bleached $0.9 \pm 2.9\%$) and the values were homogeneous throughout the cell (Fig. 1B; Fig. 1C, lower row). We therefore concluded that the FRET response of the FERM sensor was indeed intramolecular, confirming that a conformational change in the FERM domain was the underlying basis for the sensor response.

Functional characterization of the FERM sensor

We validated the reliability of the FERM sensor as an indicator of the molecular behavior of FAK during its adhesion-dependent activation in living cells by comparing its activity and behavior to that of wild-type (wt) FAK expressed in *FAK*^{-/-} fibroblasts. The null-background of *FAK*^{-/-} cells allowed a rigorous validation of physiological activity, preventing possible cross-phosphorylation and activation by endogenous protein. FAK deficiency in *FAK*^{-/-} cells leads to a rounded phenotype with an increase in the number and size of FAs, which take the form of peripherally and ventrally localized patches, and the phenotype is associated with reduced migration (Ilic et al., 1995). The FERM sensor was targeted to FAs and rescued the cell morphology, resulting in a spreading phenotype displaying typical FAs at the periphery (Fig. 1 and data not shown).

Moreover, the FERM sensor was able to rescue the migration deficiency of *FAK*^{-/-} fibroblasts towards a haptotactic stimulus to the same extent as GFP-wtFAK (Fig. 2A). The migration efficiency of transfected fibroblasts, enriched by FACS, was examined on a fibronectin matrix in Thincert chambers. No difference was

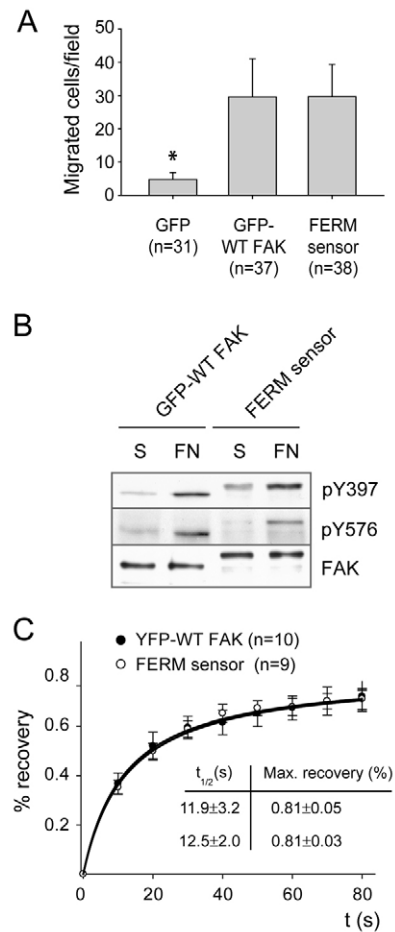


Fig. 2. Functional characterization of the FERM sensor. (A) The FERM sensor rescues *FAK*^{-/-} cell motility: the number of cells migrating through the fibronectin-coated filter of a Thincert chamber after 6 hours is shown for cells expressing GFP, GFP-wtFAK or the FERM sensor. Results are the average of three separate experiments; *n*, number of counted fields. (B) Western blot analysis of Tyr397 and Tyr576 phosphorylation for GFP-wtFAK and the FERM sensor in *FAK*^{-/-} cells. Serum-starved cells were grown on fibronectin (FN) for 24 hours or kept in suspension (S) for 1 hour. (C) FRAP analysis of cells expressing YFP-wtFAK or the FERM sensor shows identical turnover and recovery between the two.

observed in the number of migrated cells expressing the FERM sensor or GFP-wtFAK. Furthermore, the motility in both conditions was significantly elevated (by sixfold; $P < 0.001$) compared with that in GFP-expressing control cells.

The FERM sensor closely matched the molecular activation properties of wtFAK (Fig. 2B). Western blot analysis confirmed that the key regulatory sites Tyr397 and Tyr576 become phosphorylated during cell adhesion on fibronectin in cells expressing the FERM sensor. Furthermore, the phosphorylation of both sites was reduced when the cells were held in suspension, both in cells expressing the FERM sensor and those expressing GFP-wtFAK. These results demonstrate that the insertion of CFP in the FERM-KD linker does not affect the adhesion-dependent phosphorylation behavior of FAK.

Finally, FRAP analysis revealed that the FERM sensor exhibited turnover kinetics that were indistinguishable from those of YFP-wtFAK (Fig. 2C). As phosphorylation of FAK at Tyr397 determines its residence time at FAs (Hamadi et al., 2005), any alteration in

activity or phosphorylation would have become apparent from a change in the turnover rate. The identical turnover rate also excludes compensation of a potentially impaired FERM-sensor function by adaptation of turnover rates in FAs.

Having demonstrated that the FERM sensor mirrors wtFAK in terms of activity and cellular functioning, we proceeded to investigate conformational changes in the FERM domain of FAK in cells.

Integrin-mediated conformational changes in the FERM domain during cell spreading

Quantification of FRET distributions between FAs and cytosol for multiple cells that adhere to fibronectin, and statistical analysis by Kolmogorov-Smirnov (KS) testing (Fig. 3A, lower panel; Fig. 3B) revealed higher FRET efficiencies in FAs ($16.3 \pm 4.8\%$ vs $11.2 \pm 4.2\%$ in the cytosol, $P < 0.001$).

To investigate the dependence of FA-associated high FRET efficiencies on integrin-mediated adhesion and activation, *FAK*^{-/-} fibroblasts expressing the FERM sensor were held in suspension and re-plated on poly-L-ornithine (PLO) (Fig. 3A, upper panel). The measured FRET efficiencies ($6.7 \pm 4.8\%$) were significantly ($P < 0.001$) lower than in cells adhering to fibronectin, as seen from the distribution shift in the cumulative histogram and its KS analysis (Fig. 3B). We concluded that conformational changes in the FERM

domain are induced upon activation of integrins and the formation of FAs.

Although serum stimulation did not significantly alter the sensor response (data not shown), showing that the FERM conformational response is selective for integrin-ECM signaling, the experiments were mainly performed in serum-starved cells to isolate integrin signaling from other stimulatory factors. The FRET efficiencies in the cytosol of adherent cells were significantly higher than in the minimally active suspension cells on PLO (Fig. 3B). Similar results were obtained in another cell line (HEK-293, data not shown).

The time course of the integrin-mediated FERM conformational change was followed by ratiometric imaging during the spreading of REF-52 cells on fibronectin (Fig. 4). As a control, cells were allowed to adhere to PLO. After 30 minutes on fibronectin, cells were adherent and displayed a round morphology and new peripheral FAs exhibiting high FRET ratios. By contrast, cells on PLO did not show any FAs or an increase in FRET. At 60 minutes, the cells on fibronectin began to assume a more elaborate polarized shape, although most remained round. At this time point, the proportion of FAs displaying high FRET was slightly lower and was significantly reduced after 3 hours of plating (Fig. 4B). At 7 hours and later, cells were fully spread and polarized, and again showed a robust FERM-sensor response. We concluded that cell spreading involves two consecutive stages of FERM-based FAK conformational change, suggesting that the FERM domain is engaged in a complex temporal regulation mechanism.

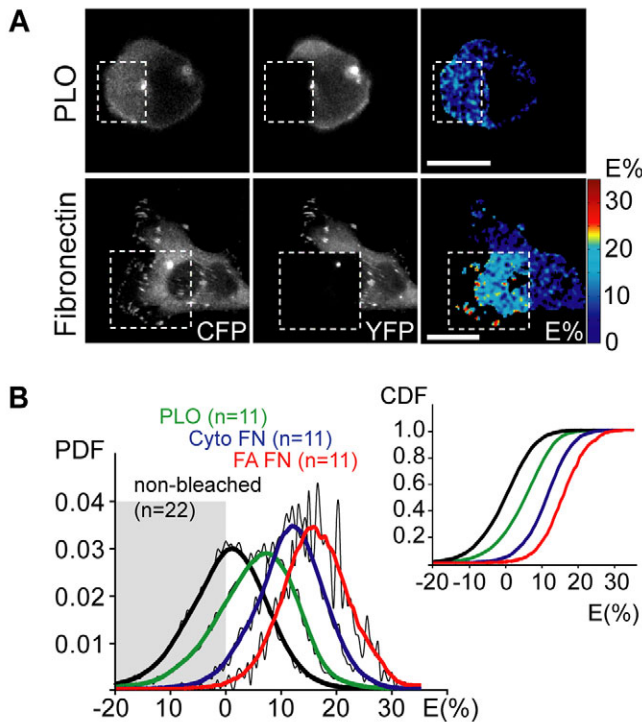


Fig. 3. The FERM sensor responds to integrin stimulation. (A) Acceptor-photobleaching FRET-efficiency (E%) images of *FAK*^{-/-} fibroblasts expressing the FERM sensor, plated on poly-L-ornithine/BSA (PLO) for 30 minutes (upper row) or on fibronectin overnight (lower row). YFP was bleached in the boxed area. FRET efficiencies are shown in pseudo-color. Scale bars: 10 μ m. (B) Cumulative FRET distribution histograms (probability density function, PDF) of PLO-plated cells, cytosol (Cyto) and FAs of fibronectin (FN)-adherent cells. Insert shows the corresponding integrated cumulative distributions (cumulative density function, CDF) for statistical analysis by KS testing, in the same color-coding.

Disruption of the regulatory KAKTLR sequence reduces adhesion-mediated conformational changes of the FERM domain

The involvement of the FERM domain in integrin-stimulated FAK activation is viewed as an auto-inhibitory interaction between the FERM domain and the KD that is released upon activation. To further delineate the mechanism of the FERM response, we introduced the K38A mutation and replaced the positively charged residues (underlined) in the KAKTLR sequence by alanine residues. The K38A mutation increased the sensor response in PLO-plated cells, but no difference in response between the native and K38A sensor was observed in fibronectin-plated cells (supplementary material Fig. S1). Although the K38A mutation destabilizes the FERM conformation of FAK, it apparently does not interfere with relevant interactions during integrin-mediated activation of FAK in adherent cells. By contrast, the FRET efficiencies for the KAKTLR mutant were significantly reduced both in the cytosol ($P < 0.05$) and FAs ($P < 0.005$) (Fig. 5A,B). In accordance, Tyr397 and Tyr576 phosphorylation of the KAKTLR-mutated FERM probe were reduced (Fig. 6). These results showed that the adhesion-associated conformational change of the FERM domain reported by our sensor requires the basic patch of the F2 lobe of the FERM domain.

We introduced the kinase-dead Arg454 and the non-phosphorylatable Phe397 mutations into the FERM sensor and found no difference in the FRET distributions of either FAs or cytosol between *FAK*^{-/-} cells expressing these mutants and those expressing the parental FERM sensor (Fig. 5A,B). These results suggest that the adhesion-mediated conformational changes of the FERM domain do not depend on kinase activity and Tyr397 phosphorylation, and, consequently, do not depend on recruitment of downstream signaling molecules. Others have reported that the FERM domain participates in the regulation of FAK activity upstream of the phosphorylation of Tyr397 (Cohen and Guan, 2005; Cooper et al., 2003; Dunty et al., 2004; Jacamo and Rozengurt,

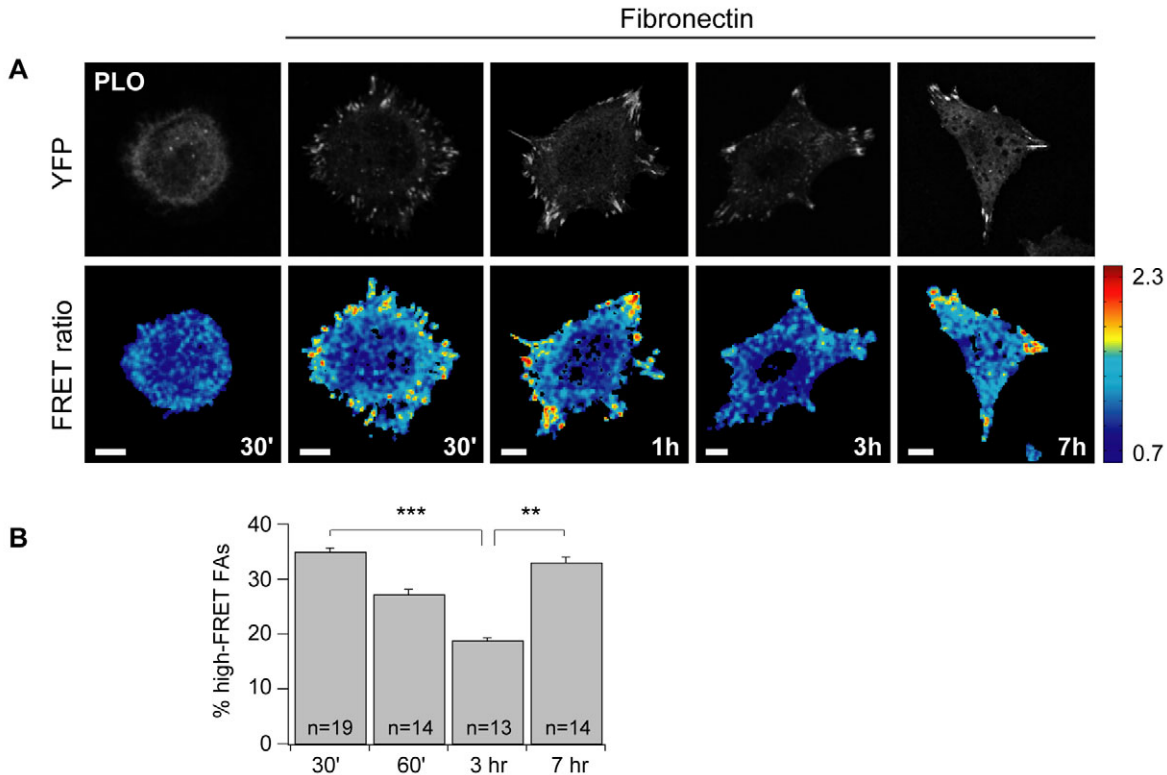


Fig. 4. Adhesion-induced conformational changes in the FERM domain of FAK during early and late phases of spreading. (A) REF-52 cells expressing the FERM sensor were held in suspension for 1 hour and were re-plated on fibronectin for the indicated time points before fixation. Cells plated on PLO for 30 minutes were taken as control. FRET was determined by ratiometric imaging. FRET ratios (YFP/CFP) are shown in pseudo-color as indicated. Scale bars: 10 μ m. (B) Proportion of FAs with FRET ratios exceeding 1.66 (60% of scale maximum), i.e. high-FRET FAs, for the different time points. Values are indicated with s.e.m.; statistical significance was tested by one-way ANOVA with Tukey post-analysis (** $P < 0.005$, *** $P < 0.001$).

2005; Lietha et al., 2007). This is in line with the reduced phosphorylation caused by KAKTLR mutation of the sensor (Fig. 6).

Correlation of FAK conformation with FA behavior

Our studies demonstrated high FRET efficiencies of the FERM sensor in FAs of adherent cells. Nevertheless, the efficiencies differed between individual loci, suggesting a relationship between FA identity and FERM conformational changes. We therefore correlated the fate of single FAs with the state of FAK, as judged by the FERM response, by ratiometric FRET imaging of living *FAK*^{-/-} fibroblasts that migrated randomly on fibronectin (Fig. 7).

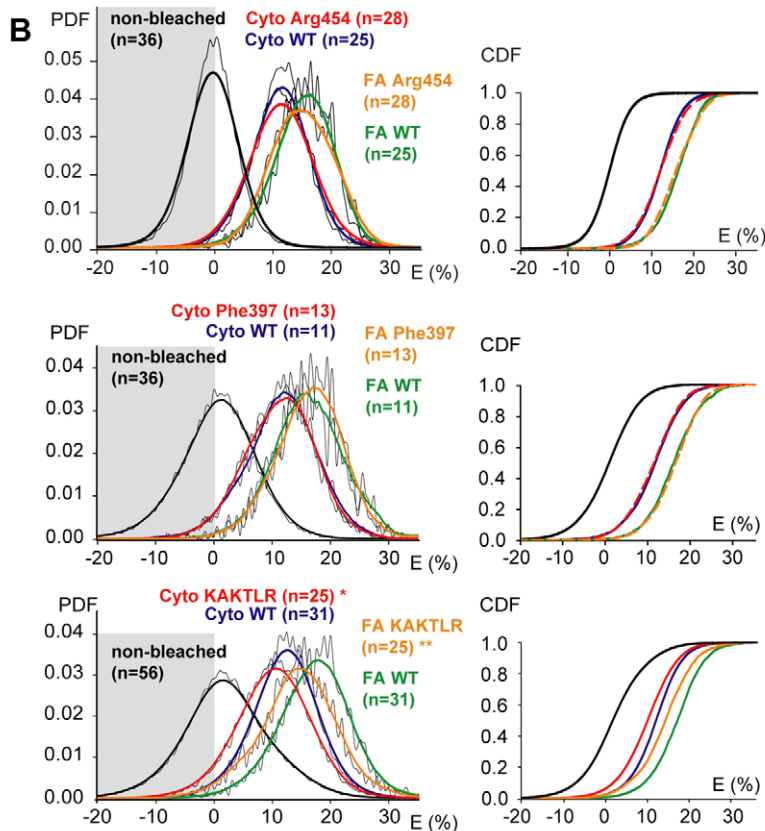
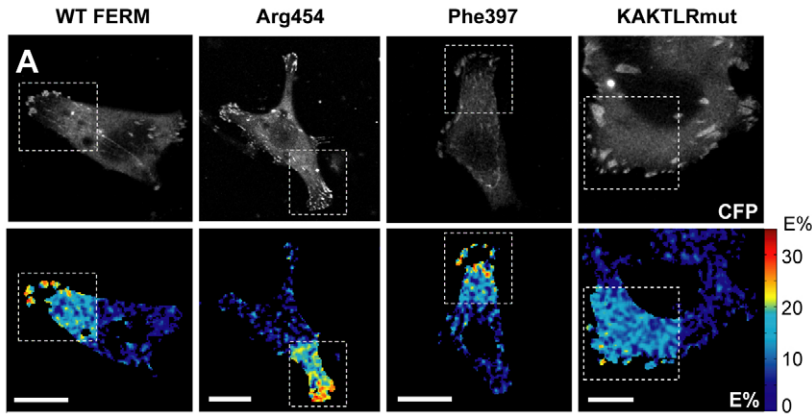
The majority of FAs showed centripetal inward sliding behavior at the retracting cell body (Fig. 7A) ($n=52$) or remained stationary (Fig. 7A; supplementary material Fig. S2) ($n=68$). We also observed FAs growing in size and/or intensity ($n=32$) at the migrating front, and shrinking ($n=25$) and/or vanishing FAs ($n=45$), mostly at the rear of the cell (supplementary material Fig. S2). The formation of new FAs was rarely seen, and was not included in the analysis. The behavior of the FERM conformation was heterogeneous, with 63% of growing FAs and 77% of sliding FAs displaying major FERM conformational changes, as indicated by high FRET ratios (Fig. 7B). By contrast, only 16% of shrinking FAs exhibited high FRET. The majority of shrinking and stationary FAs (74%) exhibited low FRET ratios, similar to those measured in the cytosol.

Because FAK is thought to be involved in gauging changes in local forces that are generated during cellular motility (Wang et al., 2001; Schober et al., 2007), we examined whether tension signaling

could contribute to the heterogeneity in FERM behavior. The generation of contractile forces for cell migration involves the phosphorylation of myosin II by Rho-associated kinase (ROCK) or myosin light-chain kinase (MLCK), with ROCK, but not MLCK, significantly affecting cellular traction forces (Beningo et al., 2006). As FAK influences both ROCK and MLCK (Ren et al., 2000; Pirone et al., 2006; Schober et al., 2007), we decided to investigate their involvement. Treatment of *FAK*^{-/-} fibroblasts expressing the FERM sensor with the ROCK inhibitor Y27632 resulted in the formation of lamellopodial extensions, and a dramatic reduction in the size and FRET efficiencies of FAs (Fig. 8C,E) ($P < 0.005$). By contrast, treatment with the MLCK inhibitor ML7 led to aberrantly oriented and often more-elongated, fibrillar FAs that showed no significant difference in FRET in comparison with untreated cells (Fig. 8B,D). The FRET response with ML7 was unaffected, even at longer incubation times (up to 45 minutes) and at high concentration (50 μ M). For both inhibitors, the FRET response in the cytosol was unchanged (data not shown). These results show that the Rho-ROCK signaling pathway can modulate the behavior of the FERM domain in FAs, and that the observed heterogeneity in FA behavior appears to involve cellular traction forces.

Discussion

A FRET-based optical biosensor for FAK was designed and used to relate conformational changes in its FERM domain to FA behavior during integrin-dependent cell spreading and migration. The sensor is based on the introduction of ECFP in the insertion-tolerant site at Val391 in the linker between the FERM domain and the KD.



The FERM sensor reveals high FRET efficiencies in FAs and low FRET efficiencies in the cytosol. Investigation of the kinetics of FERM-based conformational changes in FAK in spreading cells revealed two consecutive stages of activation, interrupted by a phase with significantly reduced FRET at around 3 hours. Furthermore, heterogeneous changes in FERM conformation were observed in individual FAs that were engaged in different behaviors during migration. The conformational change in the FERM domain of FAK was prominent in growing and sliding FAs, whereas shrinking and stable FAs appeared to predominantly contain unchanged FAK. Inhibition of intracellular contractility showed the predominant involvement of Rho-ROCK tension signaling in the modulation of the FERM response in FAs.

Deletion and mutation studies indicate that the FERM domain is involved in a complex regulation of FAK signaling (Cohen and Guan, 2005; Cooper et al., 2003; Dunty et al., 2004; Jacamo and

Fig. 5. The conformational change in the FERM domain involves the polybasic KAKTLR sequence in the F2 lobe, but is independent of intrinsic kinase activity and Tyr397 phosphorylation. (A) Acceptor-photobleaching FRET-efficiency (E%) images of *FAK*^{-/-} fibroblasts expressing the FERM sensor (WT FERM) or the Arg454 mutant, Phe397 mutant or KAKTLR mutant of the FERM sensor. YFP was bleached in the boxed area. FRET efficiencies are shown in pseudo-color. Scale bars: 10 μ m. (B) Cumulative FRET distribution histograms of the cytosol and FAs of cells expressing the Arg454 (upper), Phe397 (middle) or KAKTLR (lower) mutant FERM sensor as compared with the native (WT) FERM sensor. The corresponding integrated cumulative distributions (CDF) for statistical analysis by KS testing are shown in the right column, in the same color-coding. Statistical significance (by KS testing) of differences between mutant and native sensor in the cytosolic (Cyto) and FA compartments is indicated (* $P < 0.05$, ** $P < 0.005$).

Rozengurt, 2005). The recently reported crystal structure of the FERM-KD part of FAK supports an auto-inhibitory interaction between the FERM domain and KD (Lietha et al., 2007), suggesting the requirement of a conformational change in the FERM domain before Tyr397 can be phosphorylated. Furthermore, the inhibitory interaction was shown to involve the highly conserved basic KAKTLR sequence on the outer surface of the FERM F2 lobe. Our FERM sensor fully confirms this structural view of FAK activation because the adhesion-promoted conformational changes in the FERM domain were not affected by Lys454Arg or Tyr397Phe mutations, but were prevented by mutation of the KAKTLR sequence, which also inhibited Tyr397 phosphorylation.

During the writing of this manuscript, another FAK conformational sensor was reported that also shows the involvement of the KAKTLR sequence in a conformational response of the FERM domain (Cai et al., 2008). As in our approach, the sensor was based on the insertion of a fluorescent protein inside the FERM-KD linker to establish a FRET pair with an N-terminal fluorescent protein. However, the insertion locus was different (Arg413 vs our Val391), and the positions of donor and acceptor were switched. Surprisingly, even though the magnitude of the FRET response was comparable, it had an inverted sign.

That is, whereas the FRET signal in our FERM sensor increased with activation, a very desirable feature, it decreased with the sensor of Cai et al. upon activation.

This difference in behavior highlights an important aspect of FRET sensors that are designed to report on conformational transitions. FRET responses are most often attributed to changes in donor-acceptor separation during opening and closing of the sandwiched structure. However, we consider that it is unlikely that distance is the predominant parameter governing the FRET response with the particular sensors considered here. Because they are based on the intramolecular insertion of a fluorescent protein, greatly restricting its orientational freedom, we attribute greater importance to the influence of the 'fixed' relative dipole orientation between the FRET pair in the two conformations. The influence of dipole orientation on FRET efficiency is reflected in the κ^2 factor of the critical Förster transfer distance, R_0 ; κ^2 can vary from 0 to 4 (Jares-

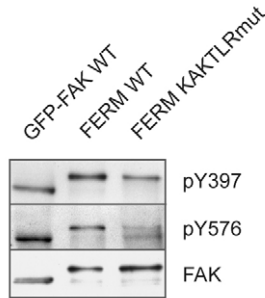


Fig. 6. KAKTLR mutation of the FERM sensor reduces Tyr397 and Tyr576 phosphorylation. Western blot analysis showing Tyr397 and Tyr576 phosphorylation of the FERM-KAKTLR mutant as compared with the native (WT) FERM sensor and GFP-wtFAK in serum-starved *FAK*^{-/-} cells that are adherent on fibronectin.

Erijman and Jovin, 2006). In support of this view, the recently published crystal structure (Lietha et al., 2007) shows that the distances between the N-terminus and insertion site Val391 in our FERM sensor and between the N-terminus and Arg413 in Cai's sensor are essentially the same. A change in separation distance should, therefore, have produced a similar response. Moreover,

exchanging the donor and acceptor in our sensor did not reverse the FRET response (data not shown). The different signs of the FRET responses of the FERM-based sensors thus argue for changes in orientation in the FERM domain rather than changes in distance. That is, the FRET response is more probably the result of a 'twisting switch' than of 'domain straightening'. A similar sign inversion has been described for two cGMP sensors based on a cGMP-dependent kinase that was N-terminally truncated at slightly different positions (Honda et al., 2001; Sato et al., 2000).

FAK activity is rapidly upregulated when cells adhere to the ECM (Schaller et al., 1994; Schlaepfer et al., 1998). Accordingly, high FRET efficiencies are found in FAs. However, integrin-mediated FAK activity is required for the opposing responses of FA formation and disassembly (Mitra et al., 2005; Parsons et al., 2000). In turn, changes in local traction forces influence FA growth and disassembly (Bershadsky et al., 2006). A complicated picture of integrin-mediated FA behavior, involving multiple signals and feedback regulation, is thus emerging. Moreover, adhesion-promoted conformational changes of the FERM domain could also be detected in cytosolic FAK, most probably as a result of its turnover between FAs and the cytosol. This result raises the intriguing possibility of integrin-mediated adhesion signaling in the cytoplasm and its regulation by cytosolic accumulation through the modulation of FAK turnover kinetics.

In order to study the regulation of FAK during haptotactic cell behavior, we investigated the conformational response of the FERM domain during spreading and random migration. We took care to exclude other stimulatory signals by mainly performing our studies under serum-depleted conditions. Cells seeded on PLO showed a sensor response that was significantly reduced as compared with fibronectin-adhering cells. This FRET response in the absence of integrin stimulation thus represents the 'resting conformation' of the FERM domain. The use of FRET imaging by acceptor photobleaching allows us to quantitatively compare the different conditions. Importantly, although the lowest-level FRET distribution for the cytoplasmic KAKTLR-mutated sensor closely matched the distribution observed in PLO-adherent cells, the non-negligible FRET efficiency present in the FAs indicated the existence of additional integrin-mediated response mechanisms.

During spreading on fibronectin, two distinct phases of FERM conformational activation could be distinguished, strongly suggesting that different regulatory mechanisms operate during initial spreading and during later, motile, phases. Around

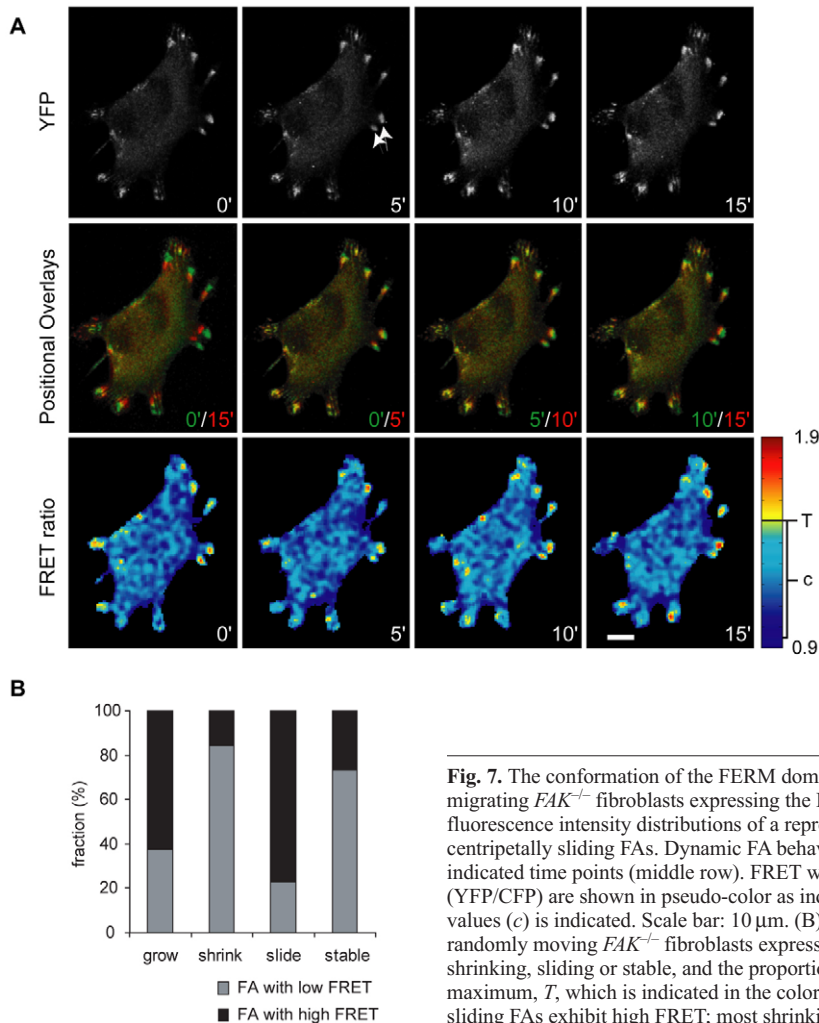


Fig. 7. The conformation of the FERM domain in FAK correlates with distinct FA behaviors. Randomly migrating *FAK*^{-/-} fibroblasts expressing the FERM sensor were imaged at 5-minute intervals. (A) YFP fluorescence intensity distributions of a representative cell (upper row). Arrows indicate examples of centripetally sliding FAs. Dynamic FA behavior is visualized by red and green overlaying of the images at the indicated time points (middle row). FRET was determined by ratiometric imaging (lower row). FRET ratios (YFP/CFP) are shown in pseudo-color as indicated. The 5th to 95th percentile FRET-ratio range of cytosol values (*c*) is indicated. Scale bar: 10 μ m. (B) Fates of 222 individual FA sites in the time-lapse images of randomly moving *FAK*^{-/-} fibroblasts expressing the FERM sensor. FA behavior was classified as growing, shrinking, sliding or stable, and the proportions of FAs with high FRET (ratios exceeding 60% of scale maximum, *T*, which is indicated in the color bar in A) were determined for each category. Most growing and sliding FAs exhibit high FRET; most shrinking and stable FAs exhibit low FRET.

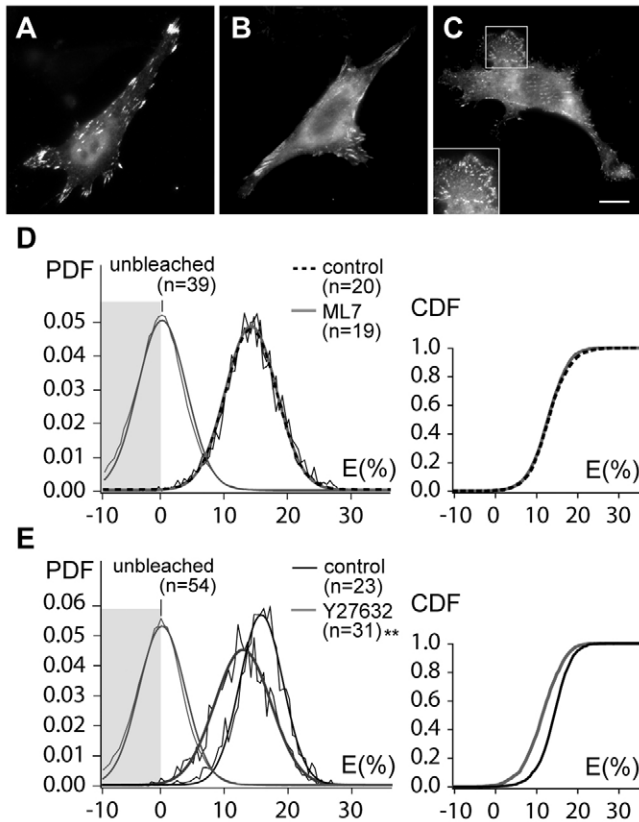


Fig. 8. ROCK-mediated tension signaling affects the conformation of the FERM domain of FAK. (A-C) YFP fluorescence intensity images of *FAK*^{-/-} fibroblasts expressing the FERM sensor: (A) untreated; (B,C) treated with either 10 μM ML7 for 20 minutes (B) or 10 μM Y27632 for 10 minutes (C). Scale bar: 10 μm. (D,E) Corresponding cumulative FRET distribution histograms (left column) and cumulative distributions for statistical analysis by KS testing (right column) as measured in FAs by acceptor photobleaching upon treatment with either ML7 (D) or Y27632 (E). Statistical significance (***P*<0.005) upon stimulation by Y27632 is indicated.

3 hours after plating, the proportion of FAs showing a strong FERM response was significantly reduced. Interestingly, the Arp2-Arp3 (Arp2/3) complex has recently been shown to interact with the FERM domain in the control of actin assembly during early cell spreading (Serrels et al., 2007). In a replating experiment, the interaction with the Arp2/3 complex was rapidly lost in *FAK*^{-/-} cells between 30 and 60 minutes of spreading. Even though the timing is different, possibly because of the different cellular backgrounds, these experiments suggest that FERM conformational regulation of FAK could involve different signaling components between newly formed and later, mature, FAs. This would be in line with the previously proposed activation mechanism (Lietha et al., 2007), according to which a conformational change in the FERM domain disrupts its interaction with the KD to allow binding of other cellular component(s). It is probable that these competing interacting components differ for the differently aged FAs.

FAs are highly heterogeneous in their molecular composition and dynamics (Ballestrem et al., 2001; Bhatt et al., 2002; Laukaitis et al., 2001; Zamir et al., 2000; Zamir and Geiger, 2001; Zimmerman et al., 2004), suggesting that different signals are triggered by the coordinated association of FAK with various interaction partners at distinct locations, leading to either formation or retraction of

adhesion sites necessary for efficient cell migration. Although the early stages of spreading and formation of adhesion sites might involve the Arp2/3 complex, Cai et al. (Cai et al., 2008) provide evidence for a regulation mechanism that involves PtdIns(4,5)*P*₂ binding to the KAKTLR sequence in the FERM-associated activation event. Furthermore, the interaction of the FERM domain with other proteins, e.g. ezrin (Pouillet et al., 2001), PIAS1 (Kadare et al., 2003), Trio (Medley et al., 2003) and activated growth-factor receptors (Chen and Chen, 2006; Sieg et al., 2000) has also been shown to regulate and modulate FAK activity. To what extent FAK-interacting proteins cooperate with integrins in the regulation of the FERM conformation remains to be determined. Heterogeneity in the activation of FAK might be further increased by post-translational modifications of the interacting proteins. For example, phosphorylation of paxillin is reduced in stationary FAs (Zaidel-Bar et al., 2007).

We observed a heterogeneous FERM conformation in mature FAs in fully adhered randomly migrating cells. Growing and sliding FAs generally showed high FRET efficiencies, whereas the majority of stable or disassembling FAs exhibited FRET efficiencies similar to those observed in the cytosol. This finding correlates with the up-to-threefold increase in integrin density and with the increase in turnover rate of sliding versus stationary FAs (Ballestrem et al., 2001), and hence a haptotactic response of FAK. Stable FAs, expected to experience constant traction forces, also showed little FAK with the altered conformation in comparison with growing and sliding FAs, considered to be the ‘towing’ sites. Thus, force signaling might contribute to the heterogeneity in the conformational response of the FERM domain, such that differential tension-dependent integrin turnover and densities lead to the observed behavioral differences.

We investigated the involvement of tension-induced signaling pathways by interfering with the phosphorylation of myosin II, using the ROCK inhibitor Y27632 and the MLCK inhibitor ML7. FAK can repress ROCK and MLCK by activation of p190RhoGAP and by the recruitment of PKL-PIX-PAK to FAs, respectively (Schober et al., 2007). Interestingly, MLCK and ROCK have been reported to play distinct roles in the regulation of fibroblast migration (Totsukawa et al., 2004). ROCK activation results in MLC phosphorylation in the center of the cell, but not at the periphery, whereas activation of MLCK has the opposite effect. Although the relationship between these mechanisms is not fully understood, it has been shown that ROCK, but not MLCK, is required for the production of traction forces in adherent cells (Beningo et al., 2006). This is in line with our findings: Y27632 treatment greatly reduced the FRET response in FAs, whereas ML7 had no effect. Our results therefore identify the Rho-ROCK pathway as a major tension-signaling route that modulates the conformational behavior of the FERM domain of FAK in FAs. The observed heterogeneous FERM response in migrating cells probably reflects different Rho-ROCK-mediated intracellular tension on individual FAs. It has been shown that active FAK represses Rho activity (Ren et al., 2000; Pirone et al., 2006; Schober et al., 2007). Conversely, a high-tension state with active Rho signaling is associated with the presence of phosphorylated FAK (Sinnott-Smith et al., 2001; Paszek et al., 2005) and, as shown here, with an altered conformation of the FERM domain of FAK. Consequently, it appears that FAK and Rho are in a dynamic balance that provides negative-feedback regulation of Rho activity and thereby controls intracellular contraction. The FERM sensor permits the spatiotemporal visualization of these dynamic mechano-regulatory processes in individual FAs.

Integrins, Rho-ROCK and FAK form a regulatory unit in the tension regulation of FAs. Independently of whether ROCK influences FAK directly or indirectly by modulation of integrin-ECM interactions, our results place the conformational change of the FERM domain of FAK at the interface between integrin and force sensing.

Materials and Methods

Construction of a FRET sensor for FAK conformational changes

The cDNA of *Gallus gallus* FAK in pEGFP-C1 (kindly provided by J. Thomas Parsons, University of Virginia, VA) was subjected to random transposon-insertion mutagenesis (Sheridan et al., 2002). For the construction of the transposon, the ampicillin-resistance gene of PUC18 (Invitrogen) was amplified by PCR, introducing terminal *NotI* and *PvuI* restriction sites that are flanked by 19-bp Tn5 mosaic ends (5'-CTGTCTCTTATACACATCT-3'), and cloned in pBlueScript. For the transposition reaction, the transposon was amplified with mosaic end primers using Pfu DNA polymerase (Promega). Equimolar amounts of the transposon and the kanamycin-resistant pEGFP-FAK vector were incubated with EZ:TN transposase (Epicentre) according to the manufacturer's instructions. XL10-Gold *Escherichia coli* (Stratagene) were transformed with the transposition mixture, and insertion clones were selected by plating on LB agar containing ampicillin (100 µg/ml) and kanamycin (50 µg/ml). The clones were subsequently screened by single-colony PCR for insertion of the transposon within the FAK cDNA and sequenced for in-frame insertions in the FERM domain and linker. The FERM sensor (YFP-FAK153-CFP) was generated by removing the ampicillin-resistance cassette of clone 153 by digestion with *NotI* and *PvuI* and substitution with ECFP flanked by the same restriction sites, generated by PCR from cCFP-CB6 (gift of Michael Way, Cancer Research UK, London). In this clone, the Tn5-flanked CFP is situated after bp 1173 (Val391). The full-length FAK sequence containing the CFP insertion was then amplified in the presence of dTTP to generate *NotI*-compatible cohesive ends and the product ligated into the *NotI* site of nYFP-CB6 (gift of Michael Way). The FAK153-CFP construct was generated by cloning the same product into pcDNA 3.1(-) (Invitrogen). For the construction of the YFP-FAK and YFP-FAK-CFP constructs, the full-length FAK cDNA was amplified from EGFP-FAK, processed as described above and ligated in the *NotI* sites of nYFP-CB6 and nYFP-cCFP CB6 vectors, respectively. Site-directed mutagenesis of YFP-FAK153-CFP was performed using the QuikChange XL site-directed mutagenesis kit (Stratagene). All constructs were confirmed by sequencing.

Cell culture and transfection

FAK^{-/-} mouse embryonic fibroblasts (MEFs) (ATCC) (Ilic et al., 1995) were cultured in DMEM containing 4.5 g/l glucose, pyruvate and Glutamax 1 (Invitrogen), 10% FCS and 1% penicillin-streptomycin in a humidified atmosphere of 5% CO₂ at 37°C. REF-52 were cultured in the same media without pyruvate. For experiments, cells were seeded on fibronectin (Sigma, 10 µg/ml) 16–24 hours before transfection at a density of 2 × 10⁵ cells per 32-mm-diameter well. Cells were transfected using the Lipofectamine 2000 reagent (Invitrogen) according to the manufacturer's instructions. Cells were serum-starved for 16 hours prior to protein analysis or imaging.

Protein analysis

Adherent cells were washed with ice-cold PBS before protein extraction in lysis buffer [10 mM Tris-HCl, pH 7.4, 100 mM NaCl, 1 mM EDTA, 1 mM EGTA, 1 mM NaF, 20 mM Na₄P₂O₇, 2 mM Na₃VO₄, 0.1% SDS, 0.5% sodium desoxycholate, 1% Tx-100, 1 mM PMSF, 10 µg/ml aprotinin, 10 µg/ml leupeptin and Protease Inhibitor Cocktail (Roche) at the recommended concentration]. Suspension cells were obtained by trypsinization, followed by washing with 1 mg/ml soybean trypsin inhibitor (Sigma) in PBS and a second wash with PBS. The cells were kept in suspension in serum-free medium in a humidified atmosphere of 5% CO₂ for 1 hour at 37°C, then centrifuged at 1500 g for 5 minutes before protein extraction. In both cases, lysis was performed on ice for 15 minutes. The resulting lysates were centrifuged at 14,000 g for 5 minutes to remove nuclei and cellular debris, and the supernatant was subjected to 7.5% SDS-PAGE and western blotting on nitrocellulose membranes. After blotting, the membranes were blocked with 5% BSA, 0.5% Tween and 2 mM Na₃VO₄ in PBS for 2 hours at 4°C, followed by incubation with anti-pY397 FAK (Biosource), anti-pY576 FAK (Biosource) or anti-FAK (BD Biosciences) antibodies at a 1:1000 dilution overnight at 4°C. Primary antibodies were detected using goat-anti-mouse and goat-anti-rabbit IgG, conjugated to horseradish peroxidase (Amersham Biosciences). Signals were visualized using enhanced chemiluminescence (ECL, Amersham Biosciences).

Cell-migration assay

FAK^{-/-} MEFs were grown and transfected in 75-cm² culture flasks. At 12–16 hours post-transfection, cells were trypsinized, resuspended in medium and sorted by GFP/YFP fluorescence using the FACSAria flow cytometer (BD Biosciences). Sorted cells were allowed to spread on fibronectin (10 µg/ml) for 2 hours and were serum-starved in medium containing 0.5% FCS for 16 hours. Thincert chambers with an 8-µm pore size (Greiner Bio-One) were coated with 20 µg/ml fibronectin and pre-

incubated in serum-free medium for 1 hour. Cells were trypsinized and washed with trypsin inhibitor before 20,000 cells per well were allowed to migrate for 6 hours. Non-migrating cells were scraped from the upper surface, and migrated cells on the lower surface of the insert were fixed with 4% formaldehyde and in ProLong/DAPI (Invitrogen). Their nuclei were counted in randomly selected fields of view. Each data point represents the average of three experiments, each including a minimum of two wells per sample, with three to seven fields analyzed from each well.

Cell treatment and imaging conditions

For acceptor photobleaching experiments, cells were fixed with 4% formaldehyde in PBS for 20 minutes, washed with 100 mM glycine in PBS and mounted in Mowiol (Sigma). For actomyosin inhibition studies, cells were treated with 10 µM Y27632 (Calbiochem) for 10 minutes or with 10 µM ML-7 (Calbiochem) for 20 minutes before fixation. For live-cell imaging, cells were placed in imaging buffer (140 mM NaCl, 5 mM KCl, 0.4 mM KH₂PO₄, 0.5 mM MgCl₂, 0.4 mM MgSO₄, 4 mM NaHCO₃, 0.1 mM Na₂HPO₄, 1.3 mM CaCl₂, 1 g/l D-glucose, 0.5 g/l BSA) and imaged using a FCS2 live-cell chamber (Biotech) at 37°C. For spreading experiments, cells were trypsinized, washed with trypsin inhibitor and re-plated for the indicated time points on coverslips that were coated with poly-L-ornithine (0.001%) and either 2% heat-denatured BSA or 10 µg/ml fibronectin.

Confocal microscopy

Cells were either imaged on a Leica DMIRE2 inverted microscope equipped with a TCS SP2 (AOBS) confocal scanner using a 63× NA 1.4 HCX PL-Apo objective (Leica) or with a FluoView1000 (Olympus) using a 60× NA 1.35 UPLS-Apo objective. CFP and YFP were excited using the 458 and 514 nm lines of the Argon laser, respectively. CFP emission was recorded at 470–505 nm and YFP at 525–590 nm. In the case of the FluoView1000, the emission channels were separated by an SDM 510 dichroic mirror.

For FRET efficiency measurements by acceptor photobleaching, images of the donor (CFP) were acquired before and after photo-destruction of the acceptor (YFP) to 15% of its original intensity in a selected region of interest. Two sequential frames were acquired and averaged for each donor image. The use of the 458 nm laser line for CFP excitation minimizes the possible occurrence of YFP photoconversion after photobleaching (Valentin et al., 2005), which was verified by imaging of cells expressing the YFP-FAK-CFP probe that lacks FRET.

For ratiometric FRET imaging in live cells, CFP and YFP fluorescence was imaged upon direct excitation by sequential line scanning for each time point without averaging. FRET is represented by the ratio YFP/CFP, which expresses the quenching of CFP emission due to FRET, normalized to the sensor concentration as given by the direct emission of YFP. The laser power was set at levels that prevented fluorophore saturation. Photomultiplier settings and laser intensities were kept constant for all images that were acquired within each experimental series to allow comparison between the different samples. For acceptor photobleaching and the ratiometric measurements, the confocal pinhole was maximally opened during acquisition to collect images with high signal:noise ratios.

For FRAP measurements, three pre-bleach images of five FAs per cell were acquired for baseline calculations at low laser power. Bleaching was performed for 10 seconds at maximum laser power. Fluorescence recovery was determined from nine images at 10-second intervals. A scan speed of 400 Hz was used during the entire experiment.

Image analysis

Image analysis was performed with the MatLab 7.0 suite (The Mathworks) using custom-written scripts. For the analysis of acceptor photobleaching experiments, donor images were binned 2 × 2 pixels, and filtered with low-pass Wiener and Gaussian filters with 3 × 3 kernel dimensions. Next, images were background-subtracted and thresholded on fluorescence intensity. FRET efficiencies were calculated on a pixel-by-pixel basis using $E = 1 - (D_{pre}/D_{post})$, where E is the FRET efficiency, and D_{pre} and D_{post} represent the CFP (donor) emission intensities before and after YFP (acceptor) photobleaching, respectively. The FRET efficiency images are represented in pseudocolor for better visualization. FRET efficiencies were separately quantified in the cytoplasm and FAs by manual selection and binary masking of peripheral FAs. These masks were used to segment the FRET efficiencies in FAs and the cytosol, i.e. the remainder of the cell. FRET-efficiency distribution histograms were normalized to the number of pixels analyzed in the corresponding areas. These were cumulated for all cells for each experimental condition, and re-normalized to the number of cells in each condition. These distributions are probability density functions (PDF), with an integral of unity. KS testing for non-Gaussian distributions was performed on the integrated cumulative distributions (cumulative density function, CDF) to estimate the statistical significance of the differences between the experimental conditions.

For the analysis of ratiometric time-lapse FRET sequences, YFP and CFP images were binned, filtered, background-subtracted and thresholded as described above for acceptor photobleaching data. Bleaching correction was not necessary because bleaching in both channels was negligible. FRET ratio signals were determined on a pixel-by-pixel basis by division of the YFP by the CFP images. The FRET-quenched CFP emission relative to the unchanged, directly excited YFP emission causes a ratio increase with increasing FRET efficiencies. Individual FAs were traced in randomly moving cells and their dynamic behavior was classified as growing, sliding, shrinking

or stable. FAs were considered to exhibit high FRET when they exceeded ratio values of 60% of the maximal signal, typically 1.3-1.5. This threshold value faithfully segments FAs with ratios that are higher than in the cytosol.

This investigation was supported by grant I/79986 of the Volkswagen Foundation to G.B., E.A.J.-E. and T.M.J. G.B. is financed by the Excellence cluster 'Microscopy at the nanometer scale' (EXC171) of the DFG Research Center for Molecular Physiology of the Brain. Y.H. participated in the International PhD Program Neurosciences, Göttingen. We thank S. van der Weijden for assistance with FRAP, J. T. Gonçalves for help with image analysis routines, W. Stühmer and C. P. Heisenberg for support, and F. S. Wouters for valuable discussions.

References

- Arold, S. T., Hoellerer, M. K. and Noble, M. E. (2002). The structural basis of localization and signaling by the focal adhesion targeting domain. *Structure* **10**, 319-327.
- Ballemstrem, C., Hinz, B., Imhof, B. A. and Wehrle-Haller, B. (2001). Marching at the front and dragging behind: differential alpha5beta3-integrin turnover regulates focal adhesion behavior. *J. Cell Biol.* **155**, 1319-1332.
- Beningo, K. A., Hamao, K., Dembo, M., Wang, Y. L. and Hosoya, H. (2006). Traction forces of fibroblasts are regulated by the Rho-dependent kinase but not by the myosin light chain kinase. *Arch. Biochem. Biophys.* **456**, 224-231.
- Bershadsky, A., Kozlov, M. and Geiger, B. (2006). Adhesion-mediated mechanosensitivity: a time to experiment, and a time to theorize. *Curr. Opin. Cell Biol.* **18**, 472-481.
- Bhatt, A., Kaverina, I., Otey, C. and Huttenlocher, A. (2002). Regulation of focal complex composition and disassembly by the calcium-dependent protease calpain. *J. Cell Sci.* **115**, 3415-3425.
- Bunt, G. and Wouters, F. S. (2004). Visualization of molecular activities inside living cells with fluorescent labels. *Int. Rev. Cytol.* **237**, 205-277.
- Burridge, K. and Fath, K. (1989). Focal contacts: transmembrane links between the extracellular matrix and the cytoskeleton. *BioEssays* **10**, 104-108.
- Cai, X., Lietha, D., Ceccarelli, D. F., Karginov, A. V., Rajfur, Z., Jacobson, K., Hahn, K. M., Eck, M. J. and Schaller, M. D. (2008). Spatial and Temporal Regulation of FAK Activity in Living Cells. *Mol. Cell Biol.* **28**, 201-214.
- Calalb, M. B., Polte, T. R. and Hanks, S. K. (1995). Tyrosine phosphorylation of focal adhesion kinase at sites in the catalytic domain regulates kinase activity: a role for Src family kinases. *Mol. Cell Biol.* **15**, 954-963.
- Ceccarelli, D. F., Song, H. K., Poy, F., Schaller, M. D. and Eck, M. J. (2006). Crystal structure of the FERM domain of focal adhesion kinase. *J. Biol. Chem.* **281**, 252-259.
- Chen, B. H., Tzen, J. T., Bresnick, A. R. and Chen, H. C. (2002). Roles of Rho-associated kinase and myosin light chain kinase in morphological and migratory defects of focal adhesion kinase-null cells. *J. Biol. Chem.* **277**, 33857-33863.
- Chen, H. C., Appeddu, P. A., Parsons, J. T., Hildebrand, J. D., Schaller, M. D. and Guan, J. L. (1995). Interaction of focal adhesion kinase with cytoskeletal protein talin. *J. Biol. Chem.* **270**, 16995-16999.
- Chen, S. Y. and Chen, H. C. (2006). Direct interaction of focal adhesion kinase (FAK) with Met is required for FAK to promote hepatocyte growth factor-induced cell invasion. *Mol. Cell Biol.* **26**, 5155-5167.
- Cohen, L. A. and Guan, J. L. (2005). Residues within the first subdomain of the FERM-like domain in focal adhesion kinase are important in its regulation. *J. Biol. Chem.* **280**, 8197-8207.
- Cooper, L. A., Shen, T. L. and Guan, J. L. (2003). Regulation of focal adhesion kinase by its amino-terminal domain through an autoinhibitory interaction. *Mol. Cell Biol.* **23**, 8030-8041.
- Dunty, J. M., Gabarra-Niecko, V., King, M. L., Ceccarelli, D. F., Eck, M. J. and Schaller, M. D. (2004). FERM domain interaction promotes FAK signaling. *Mol. Cell Biol.* **24**, 5353-5368.
- Ezratty, E. J., Partridge, M. A. and Gundersen, G. G. (2005). Microtubule-induced focal adhesion disassembly is mediated by dynamin and focal adhesion kinase. *Nat. Cell Biol.* **7**, 581-590.
- Furuta, Y., Ilic, D., Kanazawa, S., Takeda, N., Yamamoto, T. and Aizawa, S. (1995). Mesodermal defect in late phase of gastrulation by a targeted mutation of focal adhesion kinase, FAK. *Oncogene* **11**, 1989-1995.
- Gilmore, A. P. and Romer, L. H. (1996). Inhibition of focal adhesion kinase (FAK) signaling in focal adhesions decreases cell motility and proliferation. *Mol. Biol. Cell* **7**, 1209-1224.
- Girault, J. A., Labesse, G., Mornon, J. P. and Callebaut, I. (1999). The N-termini of FAK and JAKs contain divergent band 4.1 domains. *Trends Biochem. Sci.* **24**, 54-57.
- Hamadi, A., Bouali, M., Dontenwill, M., Stoeckel, H., Takeda, K. and Ronde, P. (2005). Regulation of focal adhesion dynamics and disassembly by phosphorylation of FAK at tyrosine 397. *J. Cell Sci.* **118**, 4415-4425.
- Han, D. C. and Guan, J. L. (1999). Association of focal adhesion kinase with Grb7 and its role in cell migration. *J. Biol. Chem.* **274**, 24425-24430.
- Hanks, S. K., Ryzhova, L., Shin, N. Y. and Brabek, J. (2003). Focal adhesion kinase signaling activities and their implications in the control of cell survival and motility. *Front. Biosci.* **8**, d982-d996.
- Hayashi, I., Vuori, K. and Liddington, R. C. (2002). The focal adhesion targeting (FAT) region of focal adhesion kinase is a four-helix bundle that binds paxillin. *Nat. Struct. Biol.* **9**, 101-106.
- Honda, A., Adams, S. R., Sawyer, C. L., Lev-Ram, V., Tsien, R. Y. and Dostmann, W. R. (2001). Spatiotemporal dynamics of guanosine 3',5'-cyclic monophosphate revealed by a genetically encoded, fluorescent indicator. *Proc. Natl. Acad. Sci. USA* **98**, 2437-2442.
- Hsia, D. A., Mitra, S. K., Hauck, C. R., Streblow, D. N., Nelson, J. A., Ilic, D., Huang, S., Li, E., Nemerow, G. R., Leng, J. et al. (2003). Differential regulation of cell motility and invasion by FAK. *J. Cell Biol.* **160**, 753-767.
- Ilic, D., Furuta, Y., Kanazawa, S., Takeda, N., Sobue, K., Nakatsuji, N., Nomura, S., Fujimoto, J., Okada, M. and Yamamoto, T. (1995). Reduced cell motility and enhanced focal adhesion contact formation in cells from FAK-deficient mice. *Nature* **377**, 539-544.
- Jacamo, R. O. and Rozengurt, E. (2005). A truncated FAK lacking the FERM domain displays high catalytic activity but retains responsiveness to adhesion-mediated signals. *Biochem. Biophys. Res. Commun.* **334**, 1299-1304.
- Jares-Erijman, E. A. and Jovin, T. M. (2006). Imaging molecular interactions in living cells by FRET microscopy. *Curr. Opin. Cell Biol.* **10**, 409-416.
- Kadare, G., Toutant, M., Formstecher, E., Corvol, J. C., Carnaud, M., Bouterin, M. C. and Girault, J. A. (2003). PIAS1-mediated sumoylation of focal adhesion kinase activates its autophosphorylation. *J. Biol. Chem.* **278**, 47434-47440.
- Kornberg, L., Earp, H. S., Parsons, J. T., Schaller, M. and Juliano, R. L. (1992). Cell adhesion or integrin clustering increases phosphorylation of a focal adhesion-associated tyrosine kinase. *J. Biol. Chem.* **267**, 23439-23442.
- Lauffenburger, D. A. and Horwitz, A. F. (1996). Cell migration: a physically integrated molecular process. *Cell* **84**, 359-369.
- Laukaitis, C. M., Webb, D. J., Donais, K. and Horwitz, A. F. (2001). Differential dynamics of alpha 5 integrin, paxillin, and alpha-actinin during formation and disassembly of adhesions in migrating cells. *J. Cell Biol.* **153**, 1427-1440.
- Lietha, D., Cai, X., Ceccarelli, D. F., Li, Y., Schaller, M. D. and Eck, M. J. (2007). Structural basis for the autoinhibition of focal adhesion kinase. *Cell* **129**, 1177-1187.
- Lim, Y., Han, I., Jeon, J., Park, H., Bahk, Y. Y. and Oh, E. S. (2004). Phosphorylation of focal adhesion kinase at tyrosine 861 is crucial for Ras transformation of fibroblasts. *J. Biol. Chem.* **279**, 29060-29065.
- Medley, Q. G., Buchbinder, E. G., Tachibana, K., Ngo, H., Serra-Pages, C. and Streuli, M. (2003). Signaling between focal adhesion kinase and trio. *J. Biol. Chem.* **278**, 13265-13270.
- Mitra, S. K., Hanson, D. A. and Schlaepfer, D. D. (2005). Focal adhesion kinase: in command and control of cell motility. *Nat. Rev. Mol. Cell Biol.* **6**, 56-68.
- Owen, J. D., Ruest, P. J., Fry, D. W. and Hanks, S. K. (1999). Induced focal adhesion kinase (FAK) expression in FAK-null cells enhances cell spreading and migration requiring both auto- and activation loop phosphorylation sites and inhibits adhesion-dependent tyrosine phosphorylation of Pyk2. *Mol. Cell Biol.* **19**, 4806-4818.
- Parsons, J. T., Martin, K. H., Slack, J. K., Taylor, J. M. and Weed, S. A. (2000). Focal adhesion kinase: a regulator of focal adhesion dynamics and cell movement. *Oncogene* **19**, 5606-5613.
- Paszek, W. J., Zahir, N., Johnson, K. R., Lakins, J. N., Rozenberg, G. I., Gefen, A., Reinhart-King, C. A., Margulies, S. S., Dembo, M., Boettiger, D. et al. (2005). Tensional homeostasis and the malignant phenotype. *Cancer Cell* **8**, 241-254.
- Pirone, D. M., Liu, W. F., Alom Ruiz, S., Gao, L., Raghavan, S., Lemmon, C. A., Romer, L. H. and Chen, C. S. (2006). An inhibitory role for FAK in regulating proliferation: a link between limited adhesion and RhoA-ROCK signaling. *J. Cell Biol.* **174**, 277-288.
- Poullet, P., Gautreau, A., Kadare, G., Girault, J. A., Louvard, D. and Arpin, M. (2001). Ezrin interacts with focal adhesion kinase and induces its activation independently of cell-matrix adhesion. *J. Biol. Chem.* **276**, 37686-37691.
- Reiske, H. R., Kao, S. C., Cary, L. A., Guan, J. L., Lai, J. F. and Chen, H. C. (1999). Requirement of phosphatidylinositol 3-kinase in focal adhesion kinase-promoted cell migration. *J. Biol. Chem.* **274**, 12361-12366.
- Ren, X. D., Kiosses, W. B., Sieg, D. J., Otey, C. A., Schlaepfer, D. D. and Schwartz, M. A. (2000). Focal adhesion kinase suppresses Rho activity to promote focal adhesion turnover. *J. Cell Sci.* **113**, 3673-3678.
- Ridley, A. J., Schwartz, M. A., Burridge, K., Firtel, R. A., Ginsberg, M. H., Borisy, G., Parsons, J. T. and Horwitz, A. R. (2003). Cell migration: integrating signals from front to back. *Science* **302**, 1704-1709.
- Ruest, P. J., Roy, S., Shi, E., Mernaugh, R. L. and Hanks, S. K. (2000). Phosphospecific antibodies reveal focal adhesion kinase activation loop phosphorylation in nascent and mature focal adhesions and requirement for the autophosphorylation site. *Cell Growth Differ.* **11**, 41-48.
- Sato, M., Hida, N., Ozawa, T. and Umezawa, Y. (2000). Fluorescent indicators for cyclic GMP based on cyclic GMP-dependent protein kinase alpha and green fluorescent proteins. *Anal. Chem.* **72**, 5918-5924.
- Schaller, M. D., Hildebrand, J. D., Shannon, J. D., Fox, J. W., Vines, R. R. and Parsons, J. T. (1994). Autophosphorylation of the focal adhesion kinase, pp125FAK, directs SH2-dependent binding of pp60src. *Mol. Cell Biol.* **14**, 1680-1688.
- Schlaepfer, D. D. and Hunter, T. (1996). Evidence for *in vivo* phosphorylation of the Grb2 SH2-domain binding site on focal adhesion kinase by Src-family protein-tyrosine kinases. *Mol. Cell Biol.* **16**, 5623-5633.
- Schlaepfer, D. D., Jones, K. C. and Hunter, T. (1998). Multiple Grb2-mediated integrin-stimulated signaling pathways to ERK2/mitogen-activated protein kinase: summation of both c-Src- and focal adhesion kinase-initiated tyrosine phosphorylation events. *Mol. Cell Biol.* **18**, 2571-2585.
- Schober, M., Raghavan, S., Nikolova, M., Polak, L., Pasolli, H. A., Beggs, H. E., Reichardt, L. F. and Fuchs, E. (2007). Focal adhesion kinase modulates tension signaling to control actin and focal adhesion dynamics. *J. Cell Biol.* **176**, 667-680.
- Serrels, B., Serrels, A., Brunton, V. G., Holt, M., McLean, G. W., Gray, C. H., Jones, G. E. and Frame, M. C. (2007). Focal adhesion kinase controls actin assembly

- via a FERM-mediated interaction with the Arp2/3 complex. *Nat. Cell Biol.* **9**, 1046-1056.
- Sheridan, D. L., Berlot, C. H., Robert, A., Inglis, F. M., Jakobsdottir, K. B., Howe, J. R. and Hughes, T. E.** (2002). A new way to rapidly create functional, fluorescent fusion proteins: random insertion of GFP with an in vitro transposition reaction. *BMC Neurosci.* **3**, 7.
- Sieg, D. J., Hauck, C. R. and Schlaepfer, D. D.** (1999). Required role of focal adhesion kinase (FAK) for integrin-stimulated cell migration. *J. Cell Sci.* **112**, 2677-2691.
- Sieg, D. J., Hauck, C. R., Ilic, D., Klingbeil, C. K., Schaefer, E., Damsky, C. H. and Schlaepfer, D. D.** (2000). FAK integrates growth-factor and integrin signals to promote cell migration. *Nat. Cell Biol.* **2**, 249-256.
- Sinnett-Smith, J., Lunn, J. A., Leopoldt, D. and Rozengurt, E.** (2001). Y-27632, an inhibitor of Rho-associated kinases, prevents tyrosine phosphorylation of focal adhesion kinase and paxillin induced by bombesin: dissociation from tyrosine phosphorylation of p130(CAS). *Exp. Cell Res.* **266**, 292-302.
- Tachibana, K., Sato, T., D'Avirro, N. and Morimoto, C.** (1995). Direct association of pp125FAK with paxillin, the focal adhesion-targeting mechanism of pp125FAK. *J. Exp. Med.* **182**, 1089-1099.
- Tilghman, R. W., Slack-Davis, J. K., Sergina, N., Martin, K. H., Iwanicki, M., Hershey, E. D., Beggs, H. E., Reichardt, L. F. and Parsons, J. T.** (2005). Focal adhesion kinase is required for the spatial organization of the leading edge in migrating cells. *J. Cell Sci.* **118**, 2613-2623.
- Totsukawa, G., Wu, Y., Sasaki, Y., Hartshorne, D. J., Yamakita, Y., Yamashiro, S. and Matsumura, F.** (2004). Distinct roles of MLCK and ROCK in the regulation of membrane protrusions and focal adhesion dynamics during cell migration of fibroblasts. *J. Cell Biol.* **164**, 427-439.
- Valentin, G., Verheggen, C., Piolot, T., Neel, H., Coppey-Moisan, M. and Bertrand, E.** (2005). Photoconversion of YFP into a CFP-like species during acceptor photobleaching FRET experiments. *Nat. Methods* **2**, 801.
- Wang, H. B., Dembo, M., Hanks, S. K. and Wang, Y. L.** (2001). Focal adhesion kinase is involved in mechanosensing during fibroblast migration. *Proc. Natl. Acad. Sci. USA* **98**, 11295-11300.
- Webb, D. J., Donais, K., Whitmore, L. A., Thomas, S. M., Turner, C. E., Parsons, J. T. and Horwitz, A. F.** (2004). FAK-Src signalling through paxillin, ERK and MLCK regulates adhesion disassembly. *Nat. Cell Biol.* **6**, 154-161.
- Wu, X., Suetsugu, S., Cooper, L. A., Takenawa, T. and Guan, J. L.** (2004). Focal adhesion kinase regulation of N-WASP subcellular localization and function. *J. Biol. Chem.* **279**, 9565-9576.
- Zaidel-Bar, R., Milo, R., Kam, Z. and Geiger, B.** (2007). A paxillin tyrosine phosphorylation switch regulates the assembly and form of cell-matrix adhesions. *J. Cell Sci.* **120**, 137-148.
- Zamir, E. and Geiger, B.** (2001). Molecular complexity and dynamics of cell-matrix adhesions. *J. Cell Sci.* **114**, 3583-3590.
- Zamir, E., Katz, M., Posen, Y., Erez, N., Yamada, K. M., Katz, B. Z., Lin, S., Lin, D. C., Bershadsky, A., Kam, Z. et al.** (2000). Dynamics and segregation of cell-matrix adhesions in cultured fibroblasts. *Nat. Cell Biol.* **2**, 191-196.
- Zhai, J., Lin, H., Nie, Z., Wu, J., Canete-Soler, R., Schlaepfer, W. W. and Schlaepfer, D. D.** (2003). Direct interaction of focal adhesion kinase with p190RhoGEF. *J. Biol. Chem.* **278**, 24865-24873.
- Zimmerman, B., Volberg, T. and Geiger, B.** (2004). Early molecular events in the assembly of the focal adhesion-stress fiber complex during fibroblast spreading. *Cell Motil. Cytoskeleton* **58**, 143-159.